IJES *Iranian Journal of Earth Sciences*
Vol. 13, No. 2, 2021, 115-131.

Seismic and sequence stratigraphy of the Oligocene-Miocene Asmari reservoir in the Marun oilfield, SW Iran

Jalil Jafari[1], Asadollah Mahboubi*[1], Reza Moussavi Harami[1]

1. Department of Geology, Faculty of Science, Ferdowsi University of Mashhad, Iran

Received 10 February 2020; accepted 11 July 2020

Abstract

The Oligocene-Lower Miocene Asmari Formation shows considerable reservoir heterogeneity because of variations in the lithology, depositional facies and diagenesis. This paper aim to investigate reservoir heterogeneities using seismic, core and well logs data. Twelve carbonate microfacies and three siliciclastic petrofacies are identified in the Asmari Formation based on well log and core data from 7 wells in the Marun field, which generally indicate a shallowing-up profile. Microfacies changes suggest that the Asmari Formation was deposited in a restricted lagoonal and carbonate ramp setting with periodic clastic sediment supply due to relative sea level fall. Six third-order sequences are recognized in the Asmari Formation from studies of core and well log data, while interpretation of 3D seismic data shows that the formation consists of two second-order seismic sequences. The lowest sequence boundary between the Pabdeh and Asmari Formations (SBI) is a type-2 boundary, and the six others are type-1 sequence boundaries. Six distinct packages of reflectors are interpreted on seismic data through the Cenozoic. The Pabdeh and Asmari Formations can be divided into three packages. Package 1 corresponds to transgressive and highstand systems tract deposits, which mainly consist of shales, marls, and carbonates with interbedded sandstones. This package is overlain by mounded and lenticular seismic facies (package 2) and high-amplitude and continuous seismic reflectors (package 3). Package 2 is predominantly sandstone with interbedded shale, and package3 mainly consists of carbonates. Inversion of seismic data shows that high-porosity zones are present in the western and southern Marun field. A lower high-porosity zone corresponds to lowstand fluvial-deltaic sediments and the upper zone to the beach and shallow marine sandstones.

Keywords: *Asmari Formation, Seismic packages, Sequence stratigraphy, Carbonate microfacies*

1. Introduction

The Oligocene-Lower Miocene Asmari Formation is the main oil-producing reservoir unit in SW Iran and mainly consists of carbonates with interbedded sandstones and shales. This formation overlies the Pabdeh Formation's basinal shales and carbonates and is overlain by the Gachsaran Formation's evaporites and marls. The Asmari Formation includes two members, namely, the Ahwaz Sandstone Member and Kalhur Anhydrite Member in the Khuzestan and Lurestan areas (James and Wynd 1965; Motiei 1993). The Asmari Formation can be divided into lower, middle and upper sections. Oligocene and Early Miocene ages were attributed to the lower and the middle to upper portions of the Asmari Formation respectively based on the diagnostic microfossil content respectively (James and Wynd, 1965). Adams and Bourgeois (Unpublished Report) suggested that the lower and middle sections of the Asmari Formation were deposited in the rim of an elongate basin whose borders were the Zagros main thrust to the NE (Iranian Oil Consortium Agreement Area boundary) and the preexisting Eocene platform to the SW. The deposition of the Asmari Formation occurred on the margins of a pre-existing Eocene platform that surrounded an elongate, NW-trending deep-water basin, in which the marls and deep-water limestones of the Pabdeh Formation were deposited (Ehrenberg et al. 2007). Carbonate deposition down-stepped into the Pabdeh basin (Ehrenberg et al. 2007) following a major fall in sea level near the end of the Eocene (Abreu and Anderson 1998), which corresponds to the base of megasequence AP11 (Sharland et al. 2001) (Fig 1). The deposition of the shallow-water carbonates in the middle and upper Asmari Formation continued throughout the basin through the Lower Miocene (James and Wynd 1965; Ehrenberg et al. 2007; GhasemShirazi et al. 2014; Poorbehzadi et al. 2019).

This paper investigates the Asmari Formation in the giant Marun Oilfield in the Dezful Embayment, SW Iran. This formation can be divided into five reservoir zones (10.00 to 50.00) from top to the bottom (Speers 1967, National Iranian Oil Company Unpublished report). Zones 10.00 to 40.00 consist of carbonates with sandstones at the base of each zone. Zone 50.00 at the lower part of the Asmari formation mainly consists of shales with interbedded carbonates and sandstones. The Marun Oilfield was discovered by 2D seismic data, and exploration wells were drilled in 1963. This oilfield is an NW-SE-trending asymmetrical anticline with dimensions of approximately 65×7 km on the Asmari reservoir underground contour map (Statoil and National Iranian Oil Company 2003, unpublished report). Many authors have studied the sequence stratigraphy of the Asmari Formation in the Dezful Embayment, (Vaziri-Moghaddam et al. 2006;

*Corresponding author.
E-mail address (es): mahboubi@um.ac.ir

Amirshahkarami et al. 2007; Ehrenberg et al. 2007; Van Buchem et al. 2010; Zabihi Zoeram et al. 2013; Avarjani et al. 2015; Yazdi et al. 2019; Baratian et al. 2020; Yazdi et al. 2020). However, few of these publications used seismic data to investigate the sequence stratigraphic framework of the Asmari Formation. In this paper, we study the seismic and sequence stratigraphy of the Asmari Formation at the Marun field by using 3D seismic, core and log data to investigate the depositional conditions, reservoir quality and heterogeneity in the context of the sequence stratigraphic framework.

2. Geological setting

The Zagros fold–thrust belt in SW Iran is divided into a number of NW–SE-trending structural zones that are separated by major faults, including the High Zagros and Mountain Front Faults. Laterally, the belt can be divided into the Lurestan, Dezful Embayment and Fars regions (Sepehr and Cosgrove 2004). The Marun field is located in the center of the Dezful Embayment (Fig 2).
Following the deposition of the Middle to Late Eocene Dammam Formation and its equivalents (Jahrum Formation), inversion and a eustatic sea-level fall led to widespread emergence, erosion and non-deposition across the Arabian plate (Clarke 1988; Jones and Racey 1994; Goff et al. 1995). This event corresponds to the boundary between megasequences AP10 and AP11 (Fig 1) (Sharland et al. 2001). The Pg30 maximum flooding surface (MFS) is clearly expressed across most of the plate as a surface that is close to the base of the Asmari and Kirkuk Formations (Sharland et al. 2001).

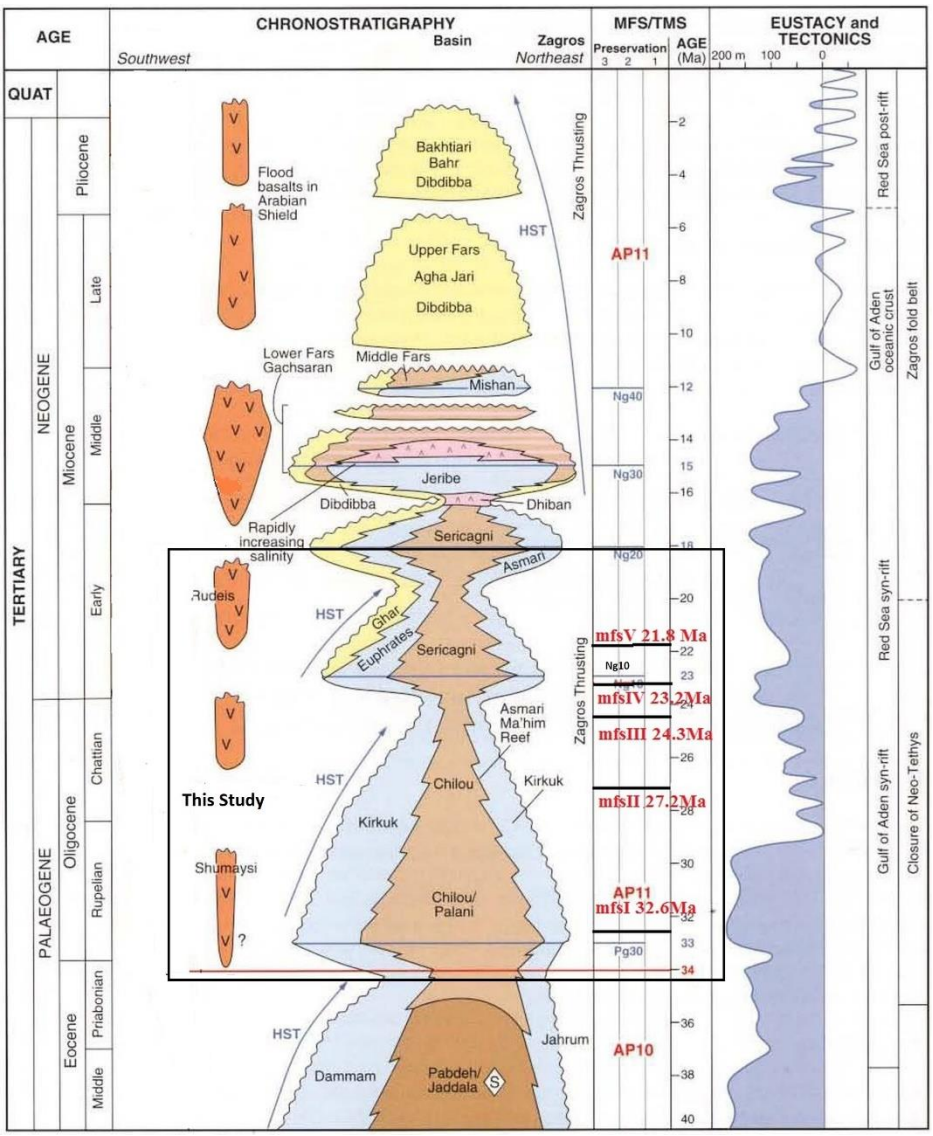

Fig 1. Schematic chronostatigraphic section for the Arabian plate's megasequence AP11, which shows the stratigraphic development of the Zagros Basin. Note the presence of two major second-order cycles sensu Vail et al. (1977). Five high-order cycles are present. The eustatic curve on the right was rescaled from Haq et al. (1988a) and is for reference only (modified after Sharland et al. 2001). MFS dating from Van Buchum et al., (2010).

Marls near the base of the Asmari limestones in Iran have been dated to the Early Oligocene (James and Wynd 1965). However, the initial marine transgression has been identified within the basinal Pabdeh Formation in southern Iran, into which the Asmari limestones prograde. Thus, the Pg30 MFS lies within the basinal sediments of the Pabdeh Formation within the foredeep area of southern Iran (Sharland et al. 2001).

The AP10-AP11 megasequence boundary coincides with the Pabdeh-Asmari boundary and corresponds to the unconformity between the Dammam-Jahrum Formations and the overlying Asmari Formation (Sharland et al. 2001). A correlative conformity can be expected to occur in basinal locations, where the Pabdeh Formation is overlain by the Asmari Formation. Towards the end of this sequence, the Zagros fold and thrust front began to develop in response to the convergence of the Arabian and Eurasian Plates, separating the foredeep basins from the Neo-Tethys Ocean.

Thus, siliciclastic sediments began to be supplied southwestwards into the basin from the emerging mountain belt (Goff et al. 1995). The Pg30 MFS at the top of the sequence AP10 records a major transgression following a brief period of emergence from a combination of inversion and eustatic sea-level fall (Haq et al. 1988).

The basin center (SW of the Zagros thrust belt) remained starved of sediment and the deposition of the fine-grained Pabdeh Formation source rock occurred (Bordenave and Burwood 1990; Jones and Racey 1994). The progressive, episodic inversion of the fold belt during the Oligocene and Miocene resulted in a number of MFSs within the reefal Asmari/Taqa/Kirkuk carbonate successions (Sharland et al., 2001). One of these MFSs, which are useful for correlation, is a calcareous shale horizon near the base of the middle Asmari limestone in Iran (Motiei, 1993). This MFS (Ng10) contains Aquitanian microfossils (Miogypsinoides-Archaias Biozone).

The Ng20 Sequence is interpreted as a third-order succession with the overlying MFS that was driven by eustasy (Fig 1). This sequence generally consists of continental siliciclastics to the west and progradational carbonates from the Asmari Formation to the east (Jones and Racey 1994). At Oligocene to Early Miocene, the Zagros Mountain thrust front was rapidly uplifted and exposed because of continuing continental collision. Thus, sediments were supplied from the emerging mountain belt to the NE, and the Arabian Plate to the SW, and formed the Ahwaz Sandstone Member (Sharland et al. 2001; Ehrenberg et al. 2007).

The Pg30 (early Oligocene-33Ma) and the Ng20 (early Miocene, mid-Burdigalian-18Ma) maximum flooding surfaces are located close to the base and in the shales below the top of the Asmari Formation respectively (Fig 1).

3. Materials and Methods

Approximately 445 m of core in the Asmari Formation from wells 8 and 342 and 1800 thin sections from cores of seven wells (8, 342, 124, 330, 30, 338, and 364) were described in terms of their carbonate lithology and texture (Dunham 1962; Embry and Klovan 1971) and sandstone petrography (Folk 1980) to investigate the depositional facies, sequence boundaries and systems tracts. Facies classification was based on the carbonate standard microfacies (SMF) of (Flugel 2010). A set of petrophysical well logs, including gamma, density and porosity logs (compensated neutron log), was used to determine the sandstone layer thickness and to interpret the depositional environments. In order to investigate sedimentary succession cycles, the Cyclolog software was used. The Cyclolog, in practice provides a state-of-the-art tool for analysis and interpretation of well logs using cluster analysis and the unique Integrate Predicate Error Filter Analysis (INPEFA) (Nio et al. 2005).

We used a set of 64-fold 3D seismic data from the Marun Oilfield to pick geological markers and perform structural interpretations, stratigraphy, architecture and depositional history of the Asmari Formation. In order to define the reservoir structure at the Marun Oilfield, we used sonic and density well logs and 16 velocity logs (checkshots and VSP) to create a synthetic seismogram and assign the correct reflectors to the geological formations. Then horizons near the tops of the Pabdeh and Asmari Formations and Gachsaran Member 6 were picked on the 3D seismic data cube. Many random, inline and crossline sections were created through a 3D seismic data cube. Three sections in the western half of the Marun field, including two inlines through wells 281 and 232 and one crossline through wells 123 and 218, were chosen for seismic stratigraphy interpretation (Fig 2). The quality of the seismic data was very low in the eastern half of the field because of the steep dip of the flanks, so no sections were chosen from this area. Then, stratal patterns were interpreted on seismic sections to recognize stratigraphic events and the depositional history.

Depositional sequences type 1 and 2 were recognized based on Posamentier et al. (1988). Parameters including reflection continuity, amplitude, frequency, interval velocity, reflection geometry and external form were used to delineate and interpret seismic facies, sequence boundaries and sequences (Sangree and Widmier 1977; Berg 1982; Van Wagoner et al. 1988; Emery and Myers 1996; Catuneanu et al. 2011). Additionally, horizon slices were cut in 10-ms intervals through a 3D attribute cube (acoustic impedance and effective porosity) to investigate the distribution of sedimentary features and high-porosity reservoir zones.

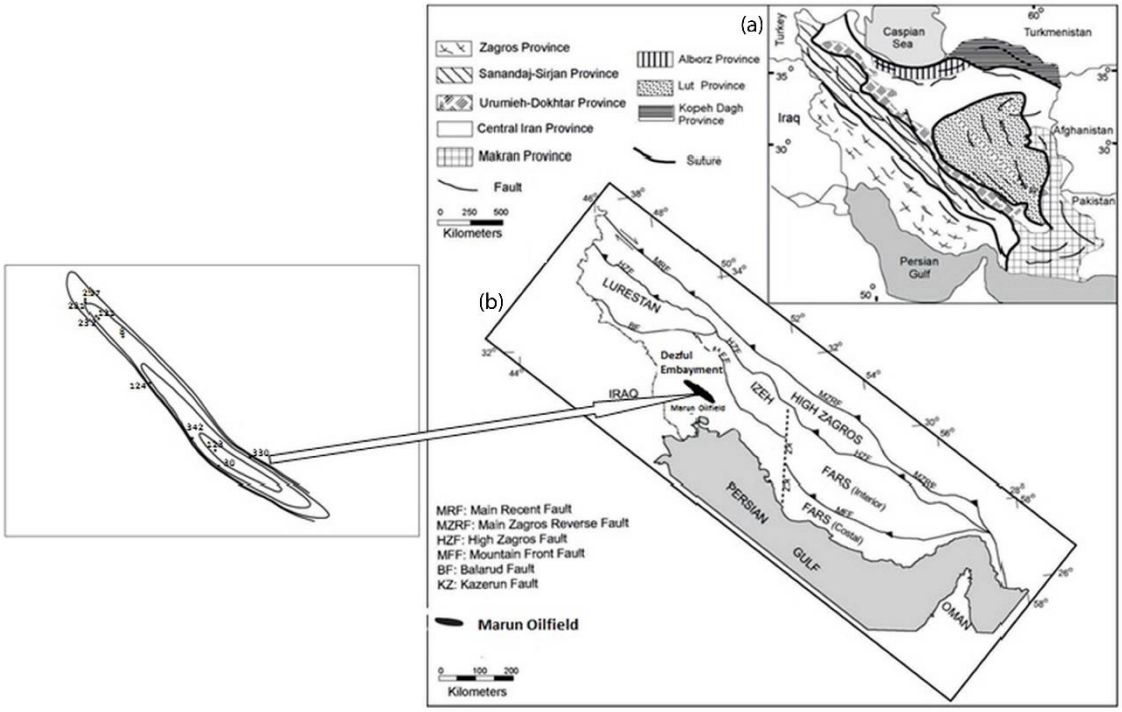

Fig 2. Location map of the studied area. a) Map of Iran that illustrates eight geological provinces (adapted from Heydari 2008). b) Subdivisions of the Zagros province. The Marun Oilfield is located in the center of the Dezful Embayment (after Farzipour et al. 2009).

4. Results

4.1. Core Petrography

Twelve carbonate microfacies and three siliciclastic petrofacies were recognized from core and thin section studies of the Asmari Formation in the Marun field. In order to follow the depositional sequences, the microfacies are described briefly from deepest to shallowest in the following paragraphs (Figs 3 and 7).

A. Carbonate Microfacies

4.1.1. Microfacies1: Pelagic mudstone to packstone

This microfacies consists of argillaceous limestones with about 5%, glauconite and pyrite grains up to 1mm. The fossil content is dominated by planktonic foraminifera such as *Globigerina* sp., *Globorotalia* sp. *and Textularia* sp., *Radiolarian* and shell debris (Fig 3a-c). Fossil tests are generally filled with calcite cement.

***Interpretation*:** Because of the presence of glauconite and pyrite grains, the fine-grained matrix and the presence of planktonic foraminifera, microfacies 1 have been deposited in deep-water conditions in an open shelf setting below the storm-wave base (Wilson 1975; Flugel 2010; Zabihi Zoeram et al. 2013).

4.1.2. Microfacies 2 – 3: Pelagic to large benthic foraminifera packstone to grainstone

This microfacies consists of pelagic carbonates with some pyrite, glauconite and silt- to sand-sized quartz grains. It is bounded with the basinal marls and shales of the lower Asmari Formation. This microfacies include approximately 70 percent *Globigerinids* and large benthic foraminifera such as *Lepidocyclina* sp., *Ditrupa* sp., *Operculina*, *Textularia* (1 to 5cm size) and echinoid debris within a lime mud matrix and sparry calcite cement (Figs 3b-c). The most frequent diagenetic processes are the calcification, micritization and dolomitization of bioclasts and stylolitization.

***Interpretation*:** This microfacies can be attributed to an open marine environment and deeper part of photic zone, due to its location, the diversity of fossil content and the presence of pyrite, glauconite in a mud matrix and fossil tests (Vaziri-Moghaddam et al., 2010; Allahkarampour Dill et al., 2017). It is equal to SMF-3 and 4 (Flugel 2010).

4.1.3. Microfacies 4: Boundstone

This microfacies consists of corals and other in-situ reef building organisms (sponges, bryozoans, and microbial crusts), together with coral and red algae debris (up to several centimeter) with spary calcite cement and some mud matrix sediments (Fig 3d, 10d). This microfacies can be divided into coralline framestone and algal boundstone facies. The micritization of coral and algal debris and cementation are the most frequent diagenetic processes.

***Interpretation*:** This microfacies is interpreted to have been deposited in a high-energy open platform or shelf edge setting that was sufficiently oxygenated with abundant nutrients (Wilson 1975; Vaziri-Moghaddam et al. 2010).

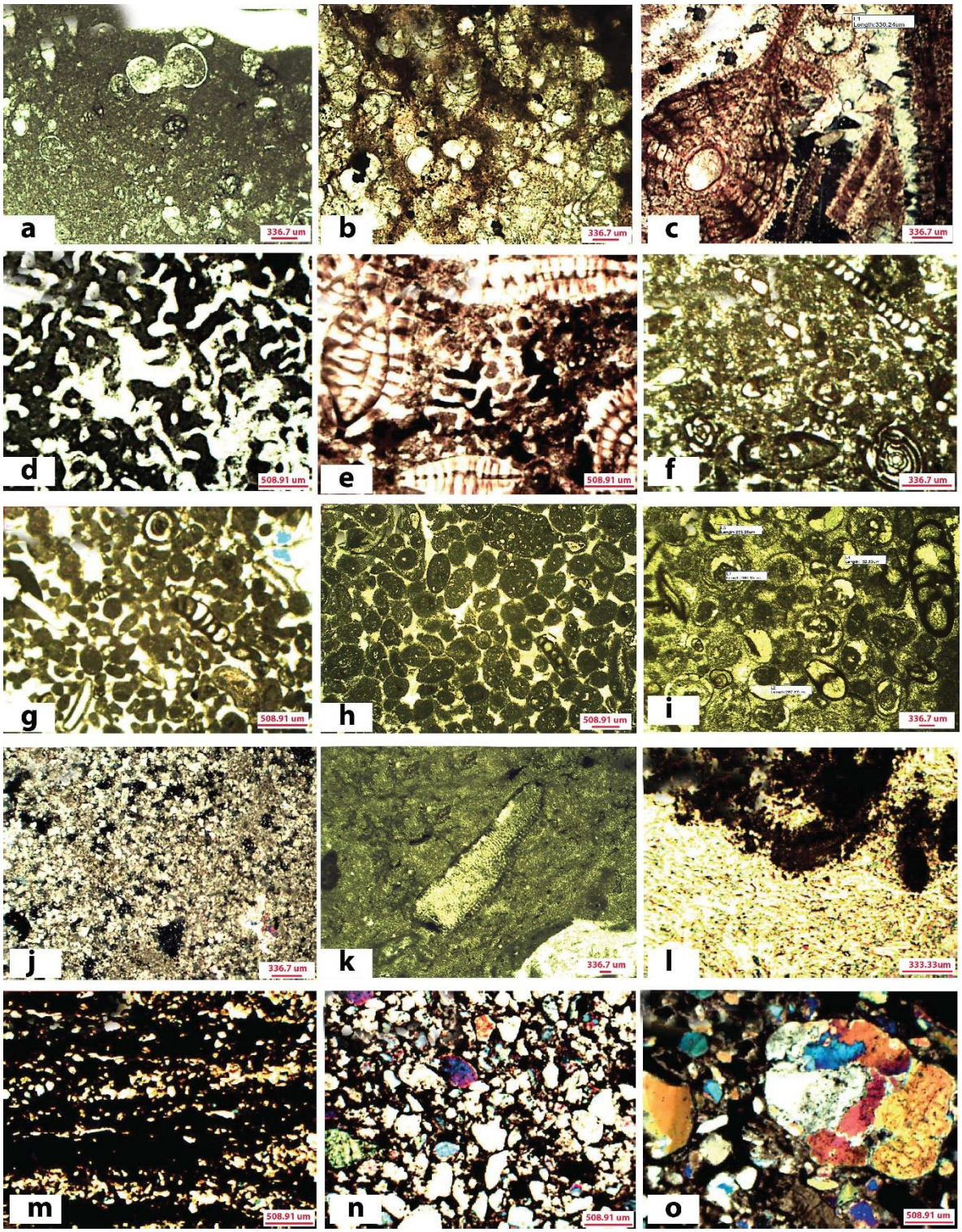

Fig 3. Depositional facies of the Asmari Formation. a. Microfacies 1, pelagic mudstone to wackestone, Well 124, depth of 3580 m; b. Microfacies 2, pelagic wackestone to packstone, Well 124, depth of 3628 m; c. Microfacies 3, pelagic-large benthic foraminifera packstone to grainstone, Well 8, depth of 12121'; d. Microfacies 4, coral boundstone, Well 8, depth of 11754'; e. Microfacies 5, bioclastic grainstone and packstone, Well 8, depth of 11,619'; f. Microfacies 6, Perforate-imperforate foraminifera wackestone to packstone, well 330, depth of 3443.5; g. Microfacies 7, imperforate foraminifera packstone to grainstone, Well 330, depth of 3384 m; h. Microfacies 8, aggregate grainstone, well 8, depth of 11,273'; i. Microfacies 9, ooid grainstone, Well 8, depth of 11241'; j. Microfacies 10, Dolostone, Well 330, depth of 3305.5 m; k. Microfacies 11, mudstone, Well 8, depth of 11034'; l. Microfacies 12, anhydrite, Well 8, of depth 11022'; m. Petrofacies 1, shale, Well 8, depth of 11926'; n. Petrofacies 2, quartz arenite, Well 8, depth of 11844'; o. Petrofacies 3, conglomerate, Well 342, depth of 3151 m. See text 4.1 for full descriptions.

The fauna content of may indicate open-marine conditions, euphotic to mesophotic zone below the base of wave action (Pomar et al., 2014; Allahkarampour Dill et al., 2017). This microfacies seems to be equal with SMF 7 (Flugel 2010, page 690),

4.1.4. Microfacies 5: Bioclastic grainstone and packstone

This microfacies contains about 70% of benthic foraminifera such as *Heterostegina* sp., *Lepidocyclina* sp., *Operculina* sp., bryozoans and 10% red algae, coral and *Rotalia* sp. with peloids and oncoids (0.5 to 2 cm) (Fig 3e). Bioclast calcification, dolomitization and micritization are the most common diagenetic processes. This microfacies mainly occurs with microfacies 4.

***Interpretation*:** Bioclastic grainstones and packstones occur as bars, channels and sand shoals in shallow lagoons and bays. Flugel (2010, SMF 5, page 686) proposed that this facies corresponds to a high-energy environment or the front of a fringing reef or inner ramp, but other authors suggested that this facies indicate deep-water, mesophotic conditions due to the presence of large, flat lepidocyclinids and nummulitids (Vaziri-Moghaddam et al. 2010; Allahkarampour Dill et al., 2017). Generally, the fauna content and clean matrix indicate high-energy and open-marine conditions.

4.1.5. Microfacies 6: Perforate-imperforate foraminifera wackestone to packstone

This microfacies contains miliolids, rotalids, *Heterostegina* sp., *Amphistegina* sp., *Peneroplis* sp., *Miogypsina* sp. *and Dendritina rangi*. The foraminifera tests are filled with dolomite and calcite cement (Fig 3f).

***Interpretation*:** The microfacies is partly dolomitized. Because of the fossil assemblage, this microfacies is interpreted to correspond to deposition in a semi-restricted to restricted lagoonal, inner platform and inner ramp setting (Flugel 2010, page 702; Allahkarampour dill et al., 2017). This microfacies may suggest shelf lagoon conditions due to the existence of open marine biota with the abundance of imperforate foraminifera such as miliolids and *Dendritina rangi* (Vaziri-Moghaddam et al., 2006; Avarjani et al, 2015).

4.1.6. Microfacies 7: Imperforate foraminifera packstone to grainstone

This microfacies mainly consists of argillaceous limestone and includes foraminifera such as miliolids, *Peneroplis* sp., *and Dendritina rangi* together with bryozoans and bivalves in a muddy matrix, with minor red algae, crinoids and crinoid fragments within a sparry calcite cement (Fig 3g).

***Interpretation*:** The faunal content suggests a variety of environments from coastal to restricted lagoon, shallow marine and euphotic zone of the inner platform setting (Pomar et al., 2014; Allahkarampour Dill et al., 2017). Bioclastic grainstones are generally deposited in an environment with constant wave or current action, which removes carbonate mud by winnowing (SMF 17) (Flugel 2010).

4.1.7. Microfacies 8: Aggregate grainstone

This microfacies consists more than 70% of oval and spherical pellets (less than 2mm diameter) with calcite cement. The grainstone and grainstone-rudstones consist of arenitic and ruditic lumps that are associated with peloids with some coated and micritized skeletal grains. Microfacies 8 include about 10% of foraminifera (*Dandritina rangi and miliolids*) tests and red algae debris (Fig 3h).

***Interpretation*:** The presence of pellets, aggregates and micritized skeletal grains suggests that this facies was deposited in low to moderate-energy conditions, such as open to restricted or shallow-marine conditions. It is equal to SMF 17 (Flugel 2010).

4.1.8. Microfacies 9: Ooid grainstone

This microfacies mainly consists of 40 to 50%, well sorted ooid grains mainly with sparry calcite cement and includes foraminifera such as *Dendritina rangi, Textularia* sp. and miliolids. The ooids are mainly less than 0.5 mm in size, and the nuclei consist of fossil fragments (Fig 3i).

***Interpretation*:** These carbonate sands with a high percentage of ooids occur near the seaward edges of platforms, banks and shelves. These sands also formed within platforms and in inner and mid-ramp settings (Mahboubi et al. 2006) suggested that the well-sorted, grain-supported texture and the lack of lime mud are diagnostic features of sediments that are deposited in high-energy settings above the fair-weather wave base. Similar sediments have been attributed to shoal environments (Wilson 1975; Flugel 2010; Vaziri-Moghaddam et al. 2010; Avarjani et al. 2015).

4.1.9. Microfacies 10: Dolostone

This microfacies consists of fine- crystalline dolomite and is mostly barren of fossils. Dolomite crystals are mainly planar with rare pellets and fossil ghosts, sometimes with authigenic evaporite minerals (Fig 3j).

Interpretation: Dolostone facies was deposited mainly with mudstone and anhydrite in a very shallow water, restricted setting (intertidal to supratidal environment) with relatively higher salinity conditions (Aqrawi et al., 2006).

4.1.10. Microfacies 11: Mudstone

This microfacies consists of mudstones and dolomitic mudstones with evaporite minerals such as anhydrite and rare miliolids, *Discorbis* sp. and fossil fragments or ghosts (Fig 3k).

***Interpretation*:** This microfacies can be interpreted to correspond to sabkha and supratidal deposition and may be the equivalent of SMF25 (Flugel 2010).The texture and fossil content of microfacies 10 and 11 are characteristic of low-energy shallow lagoons and tidal flats and saline evaporative coasts. Vaziri-Moghaddam et al. (2010) suggested that these facies indicate hypersaline conditions within a restricted lagoon.

4.1.11. Microfacies 12: Anhydrite

This microfacies consists of lath/radial crystals, nodules with 1 to 5cm diameter and thin beds of anhydrite that

are in contact with mudstone and dolo-mudstone (Fig 3l). The anhydrite facies was deposited mainly in a lime mud matrix in the uppermost part of the Asmari Formation.

***Interpretation*:** It is suggested that the anhydrite facies was deposited in a restricted evaporative environment due to occurrence with dolo-mudstone matrix (Aqrawi et al., 2006). Based on strontium dating, Ehrenberg et al. (2007) suggested that the anhydrite in the Asmari Formation formed as an evaporite deposit rather than as a later diagenetic product.

B: Siliciclastics Petrofacies

4.1.12. Petrofacies 1: Shale

This petrofacies consists of gray to black and brown, silty to sandy calcareous and fissile shales with abundance pyrite and glauconite grains. Microfossils mainly consist of planktonic foraminifera such as *Globigerina* sp., *Globorotalia* sp., with echinoid spines (Fig 3m). The amount of TOC in Asmari formation basinal shales ranges between 0.43-2.22 with an average of 1% (Opera et al. 2018, National Iranian South oil Company Unpublished Report).

***Interpretation*:** Because of the presence of planktonic microfauna with pyrite, glauconite grains and TOC content this facies is interpreted to have been deposited in reducing conditions in a deep basinal environment.

4.1.13. Petrofacies 2: Quartzarenite

Based on their texture, the sandstones can be divided as follows: fine- to medium-grained angular quartz arenites with some coarse-grained polycrystalline quartz sands with flaser bedding and ophiomorpha and skolithos ichnofossils (Figs 3n, 9d-e, 10a-c), fine- to medium-grained quartz arenites with spary calcite cement, and fine- to medium-grained quartz arenites with miliolids and bivalves debris. The last type comprises very poorly sorted, angular to rounded quartz grains with calcite cement and lime mud matrix to well-sorted and rounded fine, free quartz grains.

***Interpretation*:** The texture, sedimentary structures, fossil content, ichnofossils and gamma-log responses of these sandstones suggest deltaic, shoreline, shallow-marine and channel deposits (Figs 3n, 7, 9, 10).

4.1.14. Petrofacies 3: Conglomerates

This petrofacies consists of granule and fine pebble-sized, mainly rounded quartz clasts with calcite cement (Figs 3o, 9b-c). Conglomerates occur at the top of shallowing-upward sandstones or at the base of fining-up sandstones and occur at sequence boundaries III and IV (Figs 7, 9, see part 5.2).

***Interpretation*:** The presence of conglomerates beds at the top of sandstone cycles and the upward-coarsening gamma-log pattern in the lower portion of the Asmari Formation (Table 1) suggest the progradation of deltaic sediments into the basin, while the reverse patterns in the middle and upper portions of the formation may indicate transgressive shallow-marine, shoreline and channel settings (Catuneanu et al. 2011) (Figs 3o , 7).

4.2. Seismic Data

Six distinct packages of reflectors were interpreted from seismic data through Cenozoic.

4.2.1. Package 1

Description: This package consists of a high-amplitude, continuous set of reflectors. The thickness of this package is approximately 120 ms in two-way time (Figs 4, 5).

Interpretation: Package 1 consists of shales and pelagic mudstone to wackestones from the Pabdeh Formation and the basal portion of the Asmari Formation and corresponds to transgressive and highstand systems tracts (Figs 4a-b).

4.2.2. Package 2

Description: Wedge-shaped, mounded and sheet-like features that consist of discontinuous and low- to medium-amplitude reflectors with a thickness of approximately 130 ms in two-way time are interpreted as Package 2. This package is present in the crestal portion of the field, and in the syncline to the SW and NE of the seismic sections (Fig 4).

Interpretation: Due to wedge-shaped, mounded and sheet-like features, package 2 corresponds to transgressive, highstand and lowstand systems tracts and consists of interbedded marls, shales, limestones and fluvial-deltaic sandstones and conglomerate from the Lower Asmari Formation.

4.2.3. Package 3

Description: Package 3 consist of a set of high-amplitude, continuous reflectors which is approximately 90 ms thick. This package include the upper portion of the Asmari Formation.

Interpretation: Package 3 mainly consists of carbonates with interbedded sandstones and shales of the middle and upper Asmari Formation. Falling sea level during the Early to Middle Miocene (18.5Ma) resulted in the exposure of the Asmari Formation, and a type-1 sequence boundary formed, which can be interpreted from the seismic profiles and core data (Figs 5, 8, 9d, 9e).

4.2.4. Package 4

Description: Package 4 represents a set of mounded, chaotic and discontinuous to semi-continuous reflectors with low to high amplitude and highly variable thickness and onlap onto package 3.

Interpretation: This package is interpreted as Gachsaran Formation members 2, 3 and 4, which mainly consist of evaporites (anhydrite and salt) and lagoonal sediments (marls and argillaceous limestones). Package 4 corresponds to lowstand systems tract of the next sequence.

4.2.5. Package 5

Description: A set of high-amplitude and continuous reflectors with an average thickness of approximately 200 ms in two-way time is interpreted as package 5.

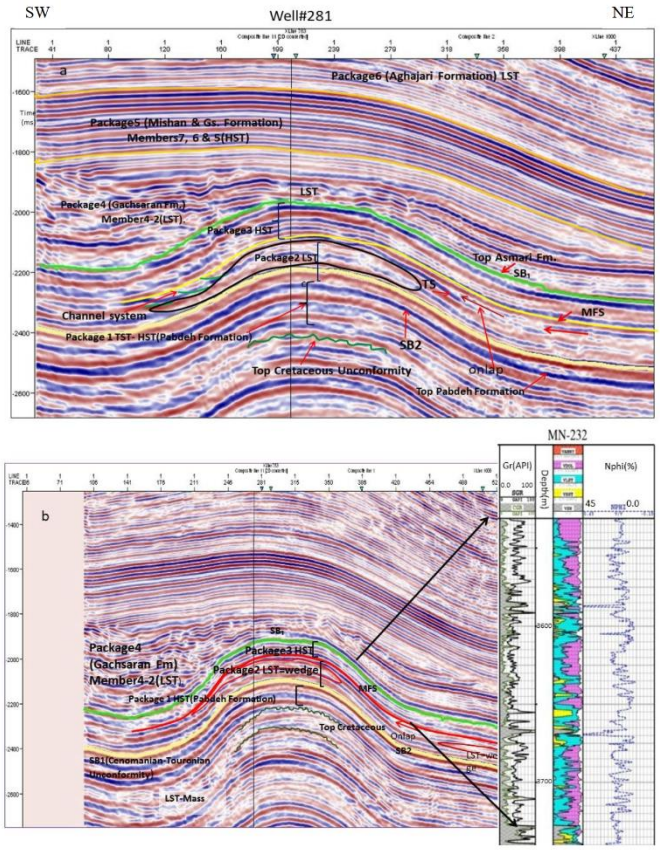

Fig 4. a. Transverse (inline) seismic section through well 281, Marun Oilfield, with interpreted seismic packages and systems tracts; b. Transverse (inline) seismic section through Well 232, Marun Oilfield, which shows the stratigraphic interpretation and the correlation among the six interpreted packages of reflectors in the seismic data and the log interpretation. Abbreviations: SB = Sequence Boundary, MFS = Maximum flooding surface, HST = Highstand systems tract, TS = Transgressive surface, TST=Transgressive systems tract, LST = Lowstand systems tract.

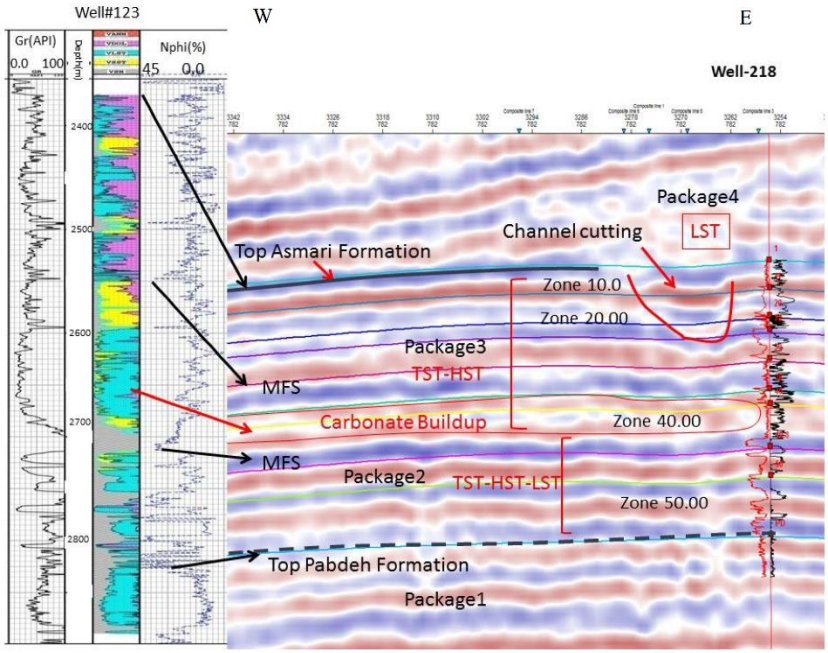

Fig 5. Longitudinal (crossline) seismic profile through wells 123 and 218, Marun Oilfield, which show the correlation among the interpreted seismic and well log data and channel cutting near top of the Asmari Formation (see Fig 8 for section line A-B and Fig 4a for abbreviations)

Table 1. Thickness and log response of the Asmari sandstone layers 30.00 and 40.00 (see Fig 7 for reservoir zonation)

Reservoir Layer	Thickness and log response of Sandstone layers 36-30, 40.00 and 40-80 in Asmari Formation(South flank)														
36-30	Well no.	381	281	302	298	293	341	243	364	342	303	371	110	312	366
	Thickness (m)	15	20	30	35	20	30	20	50m	50	45	35	25	4+4=8	12+3=15
	appearance	3Layer	3Layer	4Layer	3Layer	3Layer	3Layer	3Layer	4layer	4layer	4layer	3Layer	M. Layer	2Layer	2Layer
	Gamma log pattern	*BL	*UF/BL	UF/UC	3UF/UC	BL/UF	BL/UF	BL/UF	UF/UC	UF/UC	UF/UC	BL/UC	2UF/UC	UF/UC	UF/UC
	Environment	Estuary Channel system/ Beach-Barrier Bar Island													
40.00	Thickness (m)	40	25	35	40	25	25	40	250	150	150	80	25	shale	3m
	appearance	3layer	2layer	4layer	4layer			3layer	3layer	5layer	5layer	5layer	4layer		
	Gamma log pattern	1UC+2UF	BL/UC	1UF+3UC	UC	UC	UC	UC	UC	1UF+4UC	1UF+4UC	1UF+4UC	1UF+3UC		
	Environment	Delta lobe/Distributary Channel/ Beach-Barrier Bar Island													
40-80	Thickness (m)	N.D	10m	10m	15m	20m	25m	8	25m	20m	25m	11m	10m	10m	10m
	appearance	1	1	2Layer	1	2Layer	1	1	1layer	1layer	1layer	1layer	1layer	1layer	1layer
	Gamma log pattern	DU	DU	DU	SU	Bl/UC	Bl/UC	UC	UC	UC	BL	BL	BL	SU	SU
	Lithology			Carbonate		Sand	Sand	Sand	Sand	Sand	Sand	Sand	Sand	Carbonate	
	Environment			Mid-Ramp		Delta lobe/Submarine Fan					Submarine Fan			Mid-Ramp	

***Abbreviations: UC=Upward Coarsening, UF=Upward Fining, BL=Blocky Pattern , SU=shallowing up, DU=Deepening Up, M=Multi layer**

Interpretation: This package can be interpreted in the seismic data (Fig 4b) as Gachsaran Formation members 5, 6 and 7 (mainly consisting of anhydrite, marls and limestones with interbedded salt) and the Mishan Formation (grey marls and limestone).

4.2.6. Package 6

Description: The youngest package of variable amplitude and discontinuous to semi-continuous reflectors in the seismic data is referred to as package 6 (Figs 4a-b).

Interpretation: The Aghajari Formation, which mainly consists of red marls, sandstones and conglomerates, was deposited in the closing foreland basin because of falling sea levels during the Upper Miocene to Pliocene (Motiei 1993; Sepehr and Cosgrove 2004). This formation is equivalent to the variable amplitude and semi-continuous to discontinuous reflectors in the seismic data (package 6) (Figs 4, 5).

4.3. Inversion of seismic data

The effective porosity attribute in horizon slices shows the distribution of relatively high (9% to 11%) to very high porosity (13% to 17%) in the middle of the Asmari Formation (approximately 100 ms two-way-time (TWT) above the top of the Pabdeh Formation) in the western area of the field (Fig 6a). Various features can be defined in this horizon slice. A high effective porosity area in the elliptical plan view along the field axis may represent a barrier bar.

The distribution of high effective porosity between horizons slices 80 and 100 ms (TWT) may show the distribution of beach and barrier bar sandstones in coastal or shallow-marine settings. Given that the interval velocity of the Asmari Formation is approximately 4200 m/s, the 20 ms (TWT) interval may correspond to a sandstone interval in the middle of the Asmari Formation that is approximately 42 m thick (Figs 6a, 7). This sandstone interval has been penetrated by most of the wells in the southern flank, the crestal area and the northern flank of the field and corresponds to sandstone subzone 36.30 (Fig 7 and Table 1). This interval's thickness varies from 15 m in the western area of the field (well 381) to 50 m in the middle of the southern flank (wells 364, 342 and 303) and generally thins towards the northern (wells 286, 289 and 362) and eastern parts of the field (approximately 8 m to 15 m in wells 260, 278, 312, and 366) (Table 1).

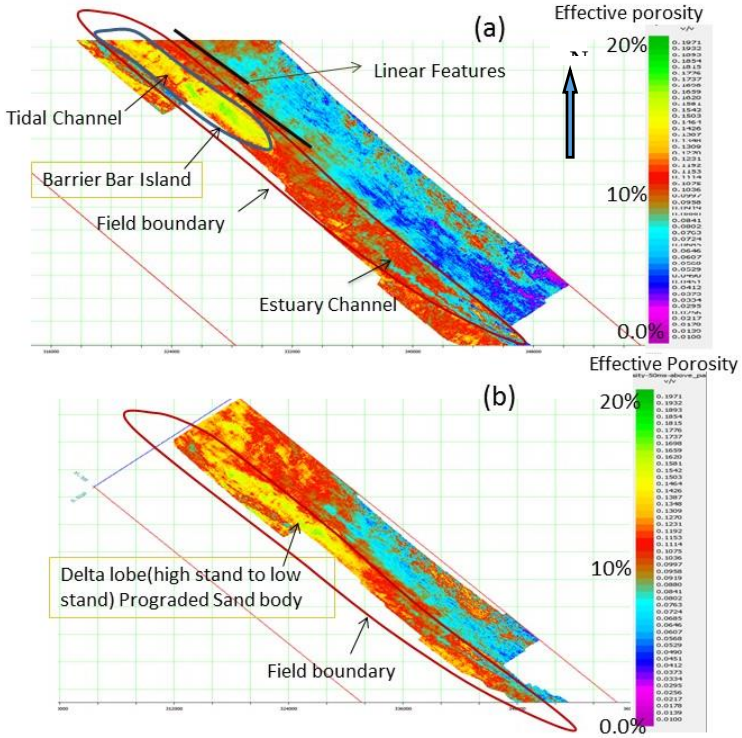

Fig 6. a. Horizon slice through an inverted 3D seismic data cube in terms of the effective porosity, which shows the distribution of beach and barrier bar sandstones in coastal or shallow-marine settings approximately 90-100 ms (TWT) above the top of the Pabdeh Formation's surface; b. Horizon slice through an inverted seismic data cube in terms of the effective porosity, which shows the possible progradation of a delta lobe sandstone approximately 40-50 ms (TWT) above the top of the Pabdeh Formation's surface.

The distribution of another high effective porosity feature between time slices 30 and 60 ms (TWT) above the top of the Pabdeh Formation's surface may represent the progradation of a fluvial-delta lobe sandstone because of falling sea levels during a late highstand to lowstand systems tract in Sequence 2 across a NW-SE-trending shoreline or in a shallow-marine environment (Fig 6b). This feature coincides with the sandstone reservoir unit 40.00 (Table 1), which have been recorded in wells 81, 232, 323, 341, 243, 364, 342, 303, 384,322, 279, 280, 312 and 366 in the southern flank of the field. This feature's thickness varies by up to 250 m in the drilled wells. The thickest sandstone interval occurs in the central area of the southern flank (250 m in well 364 and 150 m in wells 342 and 303) but thins towards the western (15.0 m in well 381), eastern (8 m in Well 312 and 12 m in well 366) and northern flanks (Table 1).

5. Discussion

5.1. Seismic Stratigraphy

5.1.1. Package 1 (HST to TST)

High amplitudes and continuous reflectors in the upper portion of the Pabdeh Formation and the basal portion of the Asmari Formation (Figs 4a, 4b, 5) suggest continuous strata that were deposited in a relatively uniform environment, and the high amplitude reflections are interpreted to indicate shales that are interbedded with relatively thick sandstones, siltstones or carbonates (c.f. Sangree and Widmier 1977). This package may be equivalent to the complex shale, carbonate and sandstone interval in the Pabdeh Formation and in reservoir zone 50.00. This package's fining-upward pattern on the gamma-ray log may correspond to a transgressive systems tract from a second-order sequence (c.f. Vail et al. 1977) (Fig 7). No evidence exists for a type-1 sequence boundary between the Pabdeh and Asmari formations in the seismic or well data at the Marun Oilfield, but a transitional interval of shales, carbonates and sandstones exists between them (Figs 4b, 5).

5.1.2. Package 2 (TST and HST to LST)

The late highstand and lowstand section of this sequence is marked by downlap, progradational reflectors and lens-like mounded features in the seismic data (Figs 4a-b, 6), which may be evidence of prograding deltaic sandstones into the Asmari Basin because of falling sea level or increasing sediment supply (c.f. Sangree and Widmier 1977). Sea level fluctuations resulted in the deposition of 3 to 5 interbedded sandstone and shale layers with an upward-coarsening pattern in the well data (reservoir zone 40.00 in Fig 7). Details of the thickness and log response of these layers are shown in Table (1). The well data show that the reservoir zones 40.00 and 50.00 mainly consist of shale and carbonate with thin layers of sandstones in the central and eastern areas of the field, so the lens-like mounded features cannot be seen over these areas (Fig 5).

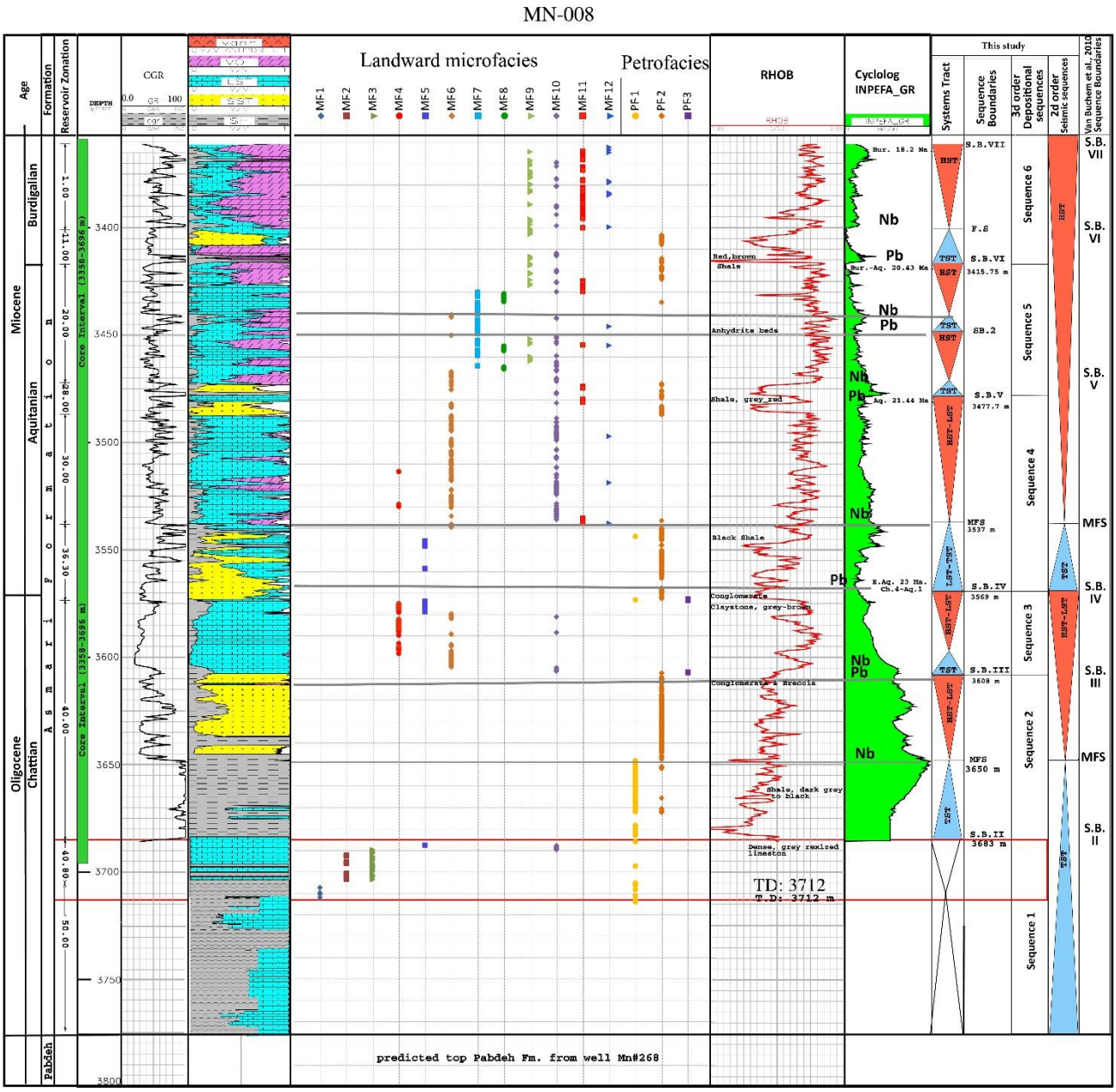

Fig 7. Key well that shows reservoir zonation, second-order seismic sequences, third-order sequences and sequence boundaries that were defined by using core and log data (this study) compared to a previous study (van Buchem et al. 2010). (See Fig 4 for abbreviations)

5.1.3. Package 3 (TST to HST)

Rising relative sea level during Early Miocene is indicated in the seismic data by a transgressive surface and onlapping reflectors on the lowstand mounded features of package2 and extends to a maximum flooding surface that can be distinguished in the seismic sections at the base of this package (Figs 4a, 4b, 5). This rising sea level resulted in the deposition of a thick layer of shallow-marine carbonates (carbonate reef), which show a mounded feature and high-amplitude and continuous reflectors throughout the Marun Oilfield (Fig 5). The thickness of this carbonate layer (microfacies 4) varies from 20 m in well 298 to 140 m in well 278. This layer's thickness is approximately 85 and 90 m in wells 123 and 218, respectively. Generally, the carbonates thicken towards the east part of the field beyond the siliciclastic sediment supply (well 312). The maximum flooding surface can be marked at the base of a high-amplitude, continuous package of reflectors, which coincide with depth 3537m in well#8 (Figs 4b, 5, 7).

The upper part of the Asmari Formation represents a package of high amplitude and continuous reflectors (55 ms, or approximately 240 m thick in well 232) and mainly consists of carbonates and sandstones with thin beds of shale (reservoir zones 30.00, 20.00 and 10.00). This package can be considered as a regressive system tract of a higher-order sequence (Fig 7).

The seismic data also show evidence for subaerial exposure and a channel system near the boundary of the Asmari and Gachsaran Formations, which may be considered a type-1 sequence boundary (Figs 5, 8) (Ashtari and Arzani 2016). This boundary was considered as a transitional boundary between lagoonal carbonates from the Asmari Formation (microfacies 9) and evaporites (anhydrite and salt) and lagoonal (marls, argillaceous limestones) deposits of the Gachsaran Formation previously; However, evidences for subaerial exposure and karstification has been reported near the boundary of the Asmari and Gachsaran Formations in the recent studies (Avarjani et al. 2015).

5.1.4. Package 4 (LST)

The chaotic to mounded pattern with semi-continuous, low- to high-amplitude reflectors and variable thickness may be attributed to the paleotopography or deformation of Gachsaran strata due to tectonic activities during Miocene to recent (Sepehr and Cosgrove, 2004). Variations in the thickness of the Gachsaran Formation may be related to Zagros orogenic movements and the accumulation of salt in synclines from Early Miocene tectonic activity (Figs 4, 5). These variations may also be related to the differential filling of semi-restricted basins with evaporites (salt and anhydrite) and marls from the Gachsaran Formation, which formed contemporaneously with tectonic movements and with the uplift of proto-anticlines in the Dezful Embayment. The onlap of the Gachsaran Formation strata onto the Asmari Formation indicates the syntectonic deposition of a lowstand systems tract during a period of rising sea level (Figs 4a, b). Package 4 could be considered the lowstand systems tract of a second-order sequence.

5.1.5. Package 5 (HST)

A rise in the relative sea level during the Early to Middle Miocene resulted in the deposition of the Gachsaran Formation (members 5, 6 and 7) and Mishan Formation. This package consists of high-amplitude, continuous reflectors of Early to Middle Miocene age and can be considered as a highstand systems tract which is rested on chaotic and discontinuous reflectors of package 4. Package 5 may suggest continuous, widespread strata that were deposited in a uniform environment (Sangree and Widmier 1977).

5.1.6. Package 6 (LST)

This package consists of semi-continuous to discontinuous and low- to high-amplitude reflectors in the upper portion of the data cube, which is equivalent to the Late Miocene- to Pliocene-age non-marine marls and sandstone layers in the Aghajari Formation (Fig 4b). Shelf seismic facies that are characterized by poor lateral continuity but with bursts of high amplitudes are typically non-marine sediment types (Sangree and Widmier 1977).

Based on age determinations (Ehrenberg et al. 2007; Van Buchem et al. 2010), the Asmari Formation was generally deposited over a period of approximately 15.4 Ma. Well data showed that this formation consists of transgressive to highstand systems tracts from a second-order sequence at the base (namely, the 50.00 reservoir zone). Generally the Asmari Formation consist of six third-order sequences, starting with siliciclastic sediments and ending with the deposition of carbonate and evaporite layers. These six third-order sequences correspond to reservoir zones 50.00 to 10.00 (Fig 7).

Seismic data interpretations showed that the Asmari Formation can be divided into two second-order depositional sequences. The lower sequence consists of a TST and an HST, while the upper section is a complete sequence with an LST, TST and HST (Figs 4, 7). Based on well logs tie with seismic data the duration of these two sequences is 15.4 Ma (Fig 5).We cannot distinguish lower order (third-order) stratigraphic sequences from the seismic data because of the poor resolution of these data; however, well log data showed four cycles of carbonates with siliciclastic sediments (sandstone and shale) at the base, which can be considered as five third-order sequences (Fig 7).

5.2. High-Resolution Sequence Stratigraphy

On a large scale, the Asmari Formation consists of transgressive and highstand systems tracts from megasequence AP11 (34 Ma-present) (Sharland et al. 2001) (Fig 1). This megasequence begins with the shales, marls and carbonates in the basal portion of the Asmari Formation as a transgressive systems tract and continues with the middle and upper Asmari limestone and sandstone layers as highstand deposits. The Fars Group (including the Gachsaran, Mishan and Aghajari formations), which constitutes a lowstand systems tract, overlies the Asmari Formation.

Ehrenberg et al. (2007) conducted a strontium isotope study of the Oligocene to Early Miocene succession (approximately 400 m thick) in the Asmari Formation in three Iranian oil fields (Ahwaz, Marun and Bi-Bi Hakimeh) and in the Kuh-e Khaviz outcrop. These authors suggested a Rupelian to Burdigalian age (34-18.5 Ma) for the Asmari Formation in the oil fields, while Sharland et al. (2001, 2004) proposed a time interval of 33.5 -19 Ma.

Van Buchem et al. (2010) identified six depositional sequences in the Asmari Formation (34-18.5 Ma). Zabihi Zoeram et al. (2013) studied the Asmari Formation in the Ghale-Nar Oilfield in the northern region of the Dezful Embayment. These authors identified four third-order depositional sequences based on the facies distributions and sequence boundaries. Six third-order depositional sequences within the Oligocene (DS1 to DS3) and Miocene (DS4 to DS6) succession from the Asmari Formation were identified in the Marun Oilfield (Avarjani et al. 2015).

In this study, six depositional sequences (five type 1 and one type 2) were recognized (*sensu* Posamentier et al. 1988) based on sedimentological data and facies distributions from core studies and well logs (INPEFA curve) (Fig 7).

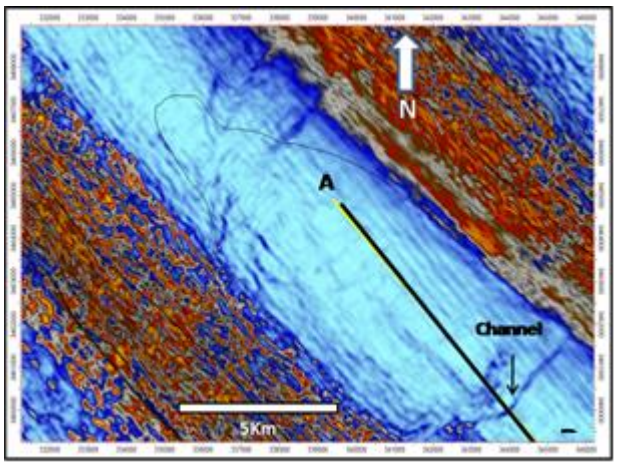

Fig 8. Spectral decomposition of 3D seismic data that shows sub-areal exposure and channel cutting near top of the Asmari Formation in the Marun Oilfield. A-B is the section line of figure 5 (modified from Ashtari and Arzani , 2016).

These sequences can be correlated with the depositional sequences (DS1 to DS6) of van Buchem et al. (2010). The age of depositional sequences1, 2 and 3 is Oligocene and depositional sequences4, 5 and 6 are identified in Early Miocene. These sequences are described below and presented in figure (7).

5.2.1. Depositional sequence1

This sequence mainly consists of dark-grey to black, silty and calcareous basinal shales, pelagic mudstones with small planktonic foraminifera (*Globigerina* sp., *Globorotalia* sp.) and pelagic wackestone to grainstones with large benthic foraminifera (*Lepidocyclina* sp., *Ditrupa* sp., *Operculina*) (microfacies 1 and 2, Figs 3a-c). This sequence corresponds to upper part of the pskage1 of the seismic data. The upper portion of this sequence has been cored in well 8 and consists of limestone. A type-2 sequence boundary (SBII) can be defined in the upper portion of this limestone layer (depth 3683 m in figure 7), which becomes silty and sandy. The limestone can be correlated with upward-coarsening and conglomeratic sandstone at a type-1 sequence boundary in the southern flank of the Marun field (SBII, well No. 342 at 3431 m, Fig 9a). The lower boundary of this sequence was not cored in well 8 and thus cannot clearly be defined, but this boundary is a type-2 boundary that can be picked out in the upper clean limestone at the top of the Pabdeh Formation in log data from other wells (Well 268). No evidence of subaerial exposure was recorded in this interval, which does not match the SBI from Van Buchem et al. (2010).

5.2.2. Depositional sequence2

Rising sea levels resulted in a maximum flooding surface at a depth of 3650 m in well No. 8 (Fig 7). This sequence consists of grey to brown and black, silty calcareous shales (Fig 3m) as TST deposits and fine to medium-grained with some subangular to rounded coarse-grained sandstones alongside conglomerate (petrofacies 2 and 3) as HST or LST deposits (Figs 3n and 3o). These sandstones show an upward-coarsening pattern in cores and an upward-cleaning pattern in the gamma-ray log and may be interpreted as delta-lobe to shallow-marine deposits (Catuneanu et al. 2011). The conglomerate layer near the top of this sandstone (depth 3608m=11838', Fig 9b) may be a type-1 sequence boundary (SBIII), which is equivalent to SBIII (about 25.1 Ma) from Van Buchem et al. (2010). Sedimentary structures such as flaser bedding (Fig 10a) and trace fossils (Skolithos and Ophiomorpha in figure 10c) support this interpretation (Seilacher, 2007). The HST and LST of this sequence in equal to the package 2 of the seismic data.

5.2.3. Depositional sequence3

Following the sea level rise at the end of sequence 2, the transgressive surface of this sequence may have been located at the top of fining-upward sandstone (depth 3607.5m, Fig 7). A carbonate platform developed in this area during TST and HST deposition. These carbonates mainly consist of grainstones and boundstones that contain large benthic foraminifera (*Lepidocyclina* sp., *Operculina* sp. *and Heterostegina* sp.), corals and red algae (microfacies 4 and 5, Figs 3d-e). The thickness of this carbonate interval varies from 20 m to the SW to 140 m (well No. 278) to the east, which is beyond the reach of siliciclastic sediments. A relative sea-level fall resulted in the formation of a thin layer of grey to brown claystones, which may be evidence for subaerial exposure and the input of siliciclastic sediments into the basin at the top of the sequence. The conglomerate at the top of the sequence can be interpreted as a type-1 sequence boundary (SBIV) at a depth of 3569 m in well 8 (Figs 7, 9c). This feature coincides with the Oligo-Miocene boundary (Chattian-Aquitanian, about 23.2 Ma) as determined by Sr isotope dating (Van Buchem et al. 2010) (Fig 7). Due to low resolution of seismic data this sequence cannot be distinguished in the seismic data.

5.2.4. Depositional sequence4

Rising relative sea levels resulted in the deposition of fining-upward cycles of sandstones and shale in coastal and shallow-marine conditions as LST to TST deposits. The maximum flooding surface was observed at a depth from 3537.3 to 3539m (Fig 7) by the presence of black and greenish to grey shales with a high gamma-ray signature on the log. Lagoonal mudstones to packstones with miliolids, *Peneroplis* sp., *Dendritina rangi* and rotalids (microfacies 6, 7 and 11, Figs 3f, 3g, 3k) and abundant nodules of anhydrite and clay seams were deposited during the HST. This sequence is terminated by 6 m of brown, fine-grained sandstones, 1.5 m of cream-colored to grey vuggy limestones and 1.5 m of red and grey to black claystones at a depth of 3477.75m in well 8 (Figs 7, 9d), which are evidence for subaerial exposure and a type-1 sequence boundary (SBV, 21.4 Ma). This sequence corresponds to lower part of the package 3.

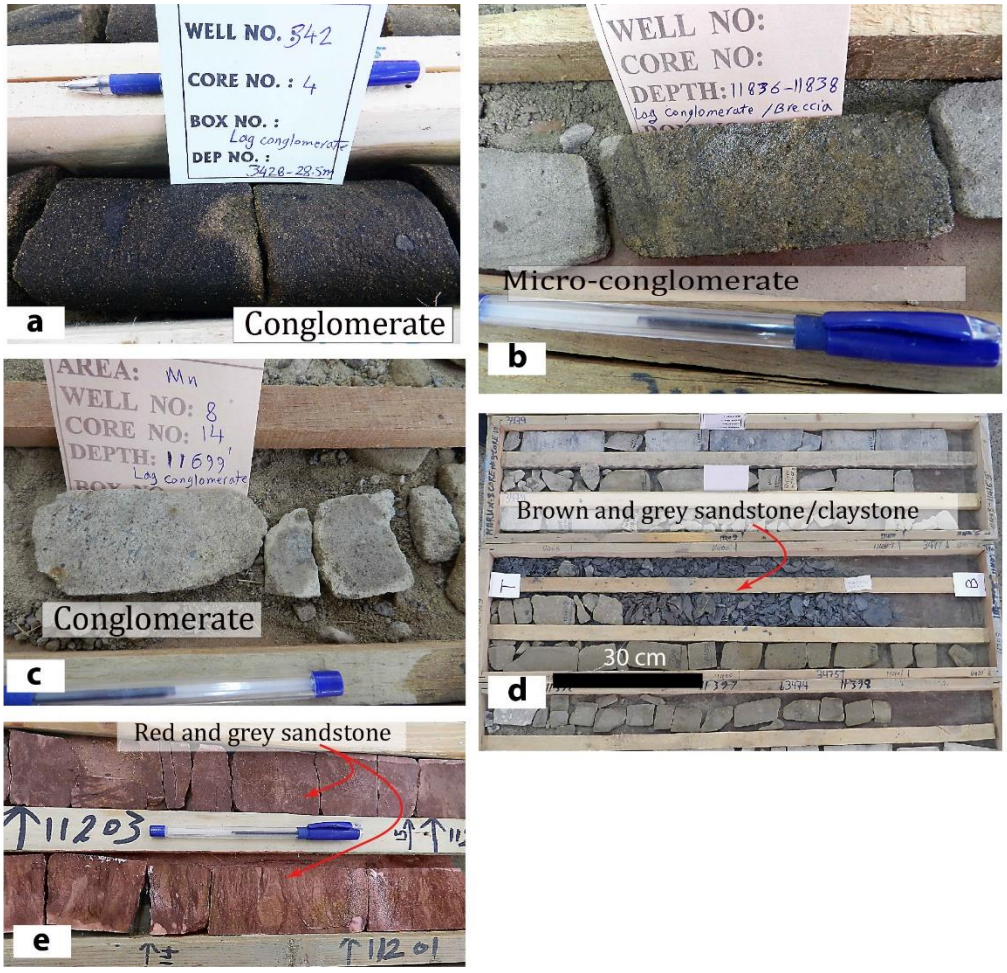

Fig 9. Sequence boundaries. a. SB II, lag conglomerate, oil saturated, Well 342, depth of 3428-31m; b. SB III, lag conglomerate and breccia, Well 8, depth 11838' (3608m); c. SB IV, lag conglomerate, Well 8, depth of 11699-10' (3569m); d. SB V, brown to grey sandstone and shale, Well 8, depth of 11400-11412' (3477m); e. SB VI, red sandstone and grey to green claystone, Well 8, depth of 11201-11204' (3415.75m).

5.2.5. Depositional sequence5

This sequence comprises brown, fine-grained sandstones and brown dolomites (Microfacies 10, Fig 3j) with anhydrite nodules (Microfacies 12) at the base, followed by cream to grey limestones with abundant anhydrite nodules and clay seams towards the top. This sequence corresponds to middle part of the package 3. The anhydrite beds (approximately 0.3 m thick at a depth of 3445 m, Figs 7, 10d, 10f) in the middle of the sequence are evidence of evaporitic conditions. The sequence can be divided into two lower-order (4th order) sequences, which are divided by the anhydrite beds (Fig 7). The upper portion of this sequence consists of cream to grey limestones (microfacies 6 and 7) with bivalves and gastropod debris and dolomites with anhydrite nodules which could be considered as TST and HST. The upper boundary is marked by thin beds of siltstone and fine-grained sandstone with 2 m of red to brown and grey to green sandstone and claystone at a depth of 3415.75 m (Fig 9e), which indicate subaerial exposure and a type-1 sequence boundary (SBVI, 20.2 Ma).

5.2.6. Depositional sequence6

This sequence consists of brown and grey vuggy dolostones (microfacies 10, Fig 3j) and brown fine-grained sandstones at the base as LST and TST deposits. The HST of this sequence consists of cream to grey and brown limestones, mainly mudstones to wackestones, with abundant anhydrite nodules (microfacies 11 and 12, Figs 3l, 10b, 10f), clay seams and bivalve and gastropod debris (Fig 10e). Sequence 6 is equal to upper portion of the package 3. The dolomites are very finely to finely crystalline and barren of microfossils and may be of supratidal and sabkha origin (Aqrawi et al. 2006). The upper boundary of this sequence with the Gachsaran Formation's evaporites is a type-1 sequence boundary (SBVII, 18.5 Ma). Evidence for subaerial exposure includes a channel system near the top of the Asmari Formation, which was distinguished in seismic data (Figs 5, 8).

Fig 10. Sedimentary characteristics of the Asmari Formation. a. Flaser bedding, Well 8, depth of 11868'; b. Anhydrite nodules, Well 8, depth of 11069-11075'; c. Trace fossils (Ophiomorpha), Well 8, Core d = 5 cm; d. Coral boundstone, Well 8, depth of 11756'; e. Bivalves, well 342, depth of 3116 m; f. Anhydrite interval, Well 8, depth of 11281-11282'.

5.3. Comparison of Seismic Sequences with High-Resolution Depositional Sequences

Only two second-order sequences could be identified with 3D seismic data. The lower sequence consists of a TST and HST (package 1). The mounded and lenticular features of package 2 begin with a lowstand systems tract at the base of the Asmari Formation and continue with a transgressive systems tract (with onlapping reflectors) in the middle. The highstand systems tract (with high-amplitude continuous reflectors from package 3) occurs in the upper portion of the Asmari Formation. A type-1 sequence boundary was defined by the channel system near the top of the Asmari Formation (Figs 5, 8) and by the onlap of the Gachsaran evaporites onto the Asmari carbonate sediments (Figs 4a, 4b).

Six depositional sequences with sequence boundaries SBI to SBVII could be recognized based on the interpretation of core and log data from wells 8 and 342. The first sequence boundary (SBI) was defined by log data from a nearby well (268) because of the lack of core data in well 8. The other sequence boundaries could be defined by both core and log data, and evidence for subaerial exposure was recognized from SBII to SBVII by using core or seismic data (Fig 7). Sequences 2 to 6 can be correlated with those from Van Buchem et al. (2010) and the age determinations of the sequence boundaries were based on strontium dating (Ehrenberg et al. 2007; Van Buchem et al., 2010).

6. Conclusions

Twelve carbonate microfacies and three siliciclastic petrofacies were identified in the Asmari Formation in the Marun Oilfield, SW Iran, which were deposited in a shallow carbonate ramp during several phases of sea level fluctuations. Six third-order depositional sequences were distinguished based on vertical and lateral facies changes and defined sequence boundaries that were recognized in core data and well logs.

Interpretations of 3D seismic data showed that the Asmari reservoir interval comprises two packages (2 and 3) of seismic reflectors. The lower portion of Package 2 can be considered the TST and HST of a second-order depositional sequence, and the upper

portion of packages 2 and 3 can be considered the LST, TST and HST of another second-order sequence. Therefore, the Asmari Formation consists of two seismic sequences in the Marun field. The first, which is located in the lower portion of the Asmari Formation, is a type-2 sequence with a TST and HST; the second is a complete type-1 sequence. A type-2 sequence boundary at the base of package 2 that overlies the Pabdeh Formation and a type-1 sequence boundary at the top of package 3 that contacts the Gachsaran Formation were distinguished by using seismic data. These seismic data also showed the presence of a lowstand wedge at the base and transgressive to highstand systems tracts in the middle and upper portions of the Asmari Formation. Lower-order sequences could not be interpreted because of the low resolution of the seismic data. The inversion of these seismic data suggested the presence of high effective porosity in the western and SW areas of the field. These areas could be related to the progradation of delta lobe sandstones into the basin during HST and LST periods (reservoir zone 40.00). The distribution of deltaic sandstone along the paleo-shoreline resulted in the presence of layer-cake sandstones throughout the field in the middle sandstone (subzone 36.30) of the Asmari reservoir.

Acknowledgements

We thank the National Iranian South Oil Company for providing seismic, well log, and core data and technical reports and the Ferdowsi University of Mashhad for their logistic and financial support during this study (project no. 3/27852).

References

Abreu VS, Anderson JB (1998) Glacial eustasy during the Cenozoic: sequence stratigraphic implications. *American Association of Petroleum Geologists Bulletin* 82:1385-1400.

Allahkarampour Dill M, Vaziri-Moghaddama H, Seyrafiana A, Behdad Ghabeishavi A (2017) Oligo-Miocene carbonate platform evolution in the northern margin of the Asmari intra-shelf basin, SW Iran. *Marine and petroleum Geology* 92:437-461.

Amirshahkarami M, Vaziri-Moghaddam H, Taheri A (2007) Paleoenvironmental model and sequence stratigraphy of the Asmari Formation in Southwest Iran. *Historical Biology* 19:173-183.

Aqrawi A, Keramati M, Ehrenberg S, Pickard N, Moallemi A, Svånå T, Darke G, Dickson J, Oxtoby N (2006) The origin of dolomite in the Asmari Formatiom (Oligocene-Lower Miocene), Dezful Embayment, SW Iran. *Journal of Petroleum Geology* 29:381- 402.

Ashtari A and Arzani A (2016) Seismic spectral decomposition and inversion for buried channels delineation: a case study from the Asmari Reservoir, southwestern Iran. *First break* 34:49-53.

Avarjani S, Mahboubi A, Moussavi-Harami R, Amiri-Bakhtiar H, Brenner RL (2015) Facies, depositional sequences, and biostratigraphy of the Oligo-Miocene Asmari Formation in Marun oilfield, North Dezful Embayment, Zagros Basin, SW Iran. *Palaeoworld* 24:336-358.

Baratian M, Arian MA, Yazdi A (2020) Petrology and Petrogenesis of Siah Kooh Volcanic Rocks in the Eastern Alborz. *Geosaberes* 11: 349-363

Berg OR (1982) Seismic detection and evaluation of delta and turbidite sequences: their application to the exploration for the subtle trap. *American Association of Petroleum Geologists Bulletin* 66:1271-1288.

Bordenave ML, Burwood R (1990) Source rock distribution and maturation in the Zagros orogenic belt, provenance of the Asmari and Bangestan reservoir oil accumulations. *Organic Geochemistry* 16:369-387.

Catuneanu O, Galloway William E, Kendall Christopher G. St. C., Miall Andrew D, Posamentier H W, Strasser A, Tucker Maurice E (2011) Sequence Stratigraphy: Methodology and Nomenclature. Newsletters on Stratigraphy 44/3: 173-245.

Clarke MWH (1988) Stratigraphy and rock unit nomenclature in the oil-producing area of Interior Oman. *Journal of Petroleum Geology* 11:5-60.

Dunham RJ (1962) Classification of carbonate rocks according to depositional textures. In: Ham, W.E., Classification of Carbonate Rocks. *American Association of Petroleum Geologists, Memoir* 1:108-121.

Ehrenberg SN, Pickard NAH, Laursen GV, Monibi S, Mossadegh ZK, Svånå TA, Aqrawi AAM, McArthur JM and Thirlwall MF (2007) Strontium isotope stratigraphy of the Asmari Formation (Oligocene-Lower Miocene), Southwest Iran. *Journal of Petroleum Geology* 30:107-128.

Embry AF, Klovan JE (1971) A late Devonian reef tract on northeastern Banks Island. *Bulletin of Canadian Petroleum Geology* 19:730-781.

Emery D, Myers K (1996) Sequence Stratigraphy. Black well science Ltd London: 297.

Farzipour S, Yassaghi A, Sherkati S.and Koyi H (2009) Basin evolution of the Lurestan region in the Zagros fold and thrust belt, Iran. *Journal of Petroleum Geology* 32:5-19.

Flugel E (2010) Microfacies of Carbonate Rocks, Analysis, Interpretation and Application. Springer-Verlag Berlin.

Folk RL (1980) Petrology of Sedimentary Rocks. Hemphill Publishing Company, Austin Texas.

GhasemShirazi B, Bakhshandeh L, Yazdi A (2014) Paleoecology of Upper Cretaceous Sediments in Central Iran, Kerman (Bondar- e Bido Section) Based on Ostracods. *Marine Science* 4 (2): 49-57

Goff JC, Jones RW, Horbury AD (1995) Cenozoic basin evolution of the northern part of the Arabian Plate and

its control on hydrocarbon habitat. *Middle East Petroleum Geosciences* 94:02-412.

Haq B, Hardenbol J, Vail P (1988) Mesozoic and Cenozoic chronostratigraphy and cycles of sea level change. In: Wilgus CK, Hastings BS, Kendall CGSC, Posamentier HW, Ross CA, Van Wagoner JC, (eds.), Sea-Level Changes: an integrated approch, *The Society of Economic Palaeontologists and Mineralogists Special Publication* 42:71-108.

Heydari E (2008) Tectonics versus eustatic control on supersequences of the Zagros Mountains of Iran. *Tectonophysics* 451:56-70.

James GA, Wynd JG (1965) Stratigraphic nomenclature of Iranian Oil Consortium Agreement Area. *American Association of Petroleum Geologists Bulletin* 49(12): 2182-2245.

Jones R, Racey A (1994) Cenozoic stratigraphy of the Arabian Peninsula and Gulf. In Simmons MD, (ed.), Micropalaeontology and Hydrocarbon Exploration in the Middle East. Chapman and Hall London.

Mahboubi A, Moussavi-Harami R, Mansouri-Daneshvar P, Nadjafi M, Brenner RL (2006) Upper Maastrichtian depositional environments and sea-level history of the Kopet-Dagh Intracontinental Basin, Kalat Formation, NE Iran. *Facies* 52:237-248.

Motiei H (1993) Stratigraphy of Zagros (Treatise on the Geology of Iran, in Persian). Geological Survey of Iran, Tehran.

Nio S, Brouwer J, Smith D, De Jong M, Böhm A (2005) Spectral trend attribute analysis, Applications in the stratigraphic analysis of wireline logs. *First Break* 23:71-75.

Pomar L, Mateu-Vicens G, Morsilli M, Brandano M, (2014) Carbonate ramp evolution during the late Oligocene (chattian), Salento peninsula, southern Italy. *Palaeogeography Palaeoclimatology Palaeoecology* 404 (0): 109-132.

Poorbehzadi K, Yazdi A, Sharifi Teshnizi E, Dabiri R (2019) Investigating of Geotechnical Parameters of Alluvial Foundation in Zaram-Rud Dam Site, North Iran. *International Journal of Mining Engineering and Technolog*y 1(1): 33-34

Posamentier HW, Jervey MT, Vail PR (1988) Eustatic controls on clastic deposition I-Conceptual framework. In: Wilgus CK, Hastings BS, Kendall CGSC, Posamentier HW, Ross CA, Van Wagoner JC, (eds.), Sea-Level Changes: an integrated approch. *Society of Economic Paleontologists and Mineralogists Special Publication* 42, Tulsa Oklahoma:110-124.

Sangree J, Widmier J (1977) Seismic interpretation of clastic depositional facies (part 9). In: Payton CE, (ed.), Seismic Stratigraphy, Applications to Hydrocarbon Exploration. *American Association of Petroleum Geologists Memoir* 26, *Tulsa Oklahoma*:165-184.

Seilacher A (2007) Trace fossil analysis. Springer-Verlag Berlin Heidelberg: 226.

Sepehr M, Cosgrove J (2004) Structural framework of the Zagros fold–thrust belt, Iran. *Marine and Petroleum Geology* 21:829-843.

Sharland P, Archer R, Casey D, Davies RB, Hall S, Heward A, Horbury A, Simmons, M., (2001) Arabian Plate Sequence Stratigraphy: *GeoArabia, Special Publication* 2, Bahrain.

Sharland PR, Casey DM, Davies RB, Simmons MD, Sutcliffe OE (2004) Arabian Plate Sequence Stratigraphy–revisions to Special Publication 2, *GeoArabia* 9:199-214.

Van Buchem F, Allan T, Laursen G, Lotfpour M, Moallemi A, Monibi S, Motiei H, Pickard N, Tahmasbi A, Vedrenne V (2010) Regional stratigraphic architecture and reservoir types of the Oligo-Miocene deposits in the Dezful Embayment (Asmari and Pabdeh Formations) SW Iran. *Geological Society London Special Publication* 329:219-263.

Van Wagoner JC, Posamentier HW, Mitchum RM, Vail PR, Sarg JF, Loutit TS, Hardenbol J (1988) An overview of the fundamentals of sequence stratigraphy and key definitions. In: Wilgus CK, Hastings BS, Posamentier H, Van Wagoner J, Ross CA, Kendall CGSC, (eds.), Sea-Level Changes: an integrated approach, *Society of Economic Palaeontologists and Mineralogists, Special Publication* 42:39-45.

Vaziri-Moghaddam H, Kimiagari M, Taheri A (2006) Depositional environment and sequence stratigraphy of the Oligo-Miocene Asmari Formation in SW Iran. *Facies* 52:41-51.

Vaziri-Moghaddam H, Seyrafian A, Taheri A and Motiei H (2010) Oligocene-Miocene ramp system (Asmari Formation) in the NW of the Zagros Basin, Iran, Microfacies, paleoenvironment and depositional sequence. *Revista Mexicana de Ciencias Geológicas* 27:56-71.

Wilson JL, (1975) Carbonate Facies in Geologic History. Springer-Verlag Berlin.

Yazdi A, Shahhosini E, Dabiri R, Abedzadeh H (2019) Magmatic differentiation evidences and source characteristics using mineral chemistry in the Torud intrusion (Northern Iran). *Revista Geoaraguaia* 9(2): 1-21

Yazdi A, Sharifi Teshnizi E (2021) Effects of contamination with gasoline on engineering properties of fine-grained silty soils with an emphasis on the duration of exposure, Springer, *SN Applied Sciences* 3:704.

Zabihi Zoeram F, Vahidinia M, Mahboubi A and Amiri Bakhtiar H (2013) Facies analysis and sequence stratigraphy of the Asmari Formation in the northern area of Dezful Embayment, south-west Iran. *Studia UBB Geologia* 58:45-56.